

## Application of Fourier Transform Spectroscopy to Magnetic Resonance

R. R. ERNST AND W. A. ANDERSON

*Analytical Instrument Division, Varian Associates, Palo Alto, California 94303*

(Received 9 July 1965; and in final form, 16 September 1965)

The application of a new Fourier transform technique to magnetic resonance spectroscopy is explored. The method consists of applying a sequence of short rf pulses to the sample to be investigated and Fourier-transforming the response of the system. The main advantages of this technique compared with the usual spectral sweep method are the much shorter time required to record a spectrum and the higher inherent sensitivity. It is shown theoretically and experimentally that it is possible to enhance the sensitivity of high resolution proton magnetic resonance spectroscopy in a restricted time up to a factor of ten or more. The time necessary to achieve the same sensitivity is a factor of 100 shorter than with conventional methods. The enhancement of the sensitivity is essentially given by the square root of the ratio of line width to total width of the spectrum. The method is of particular advantage for complicated high resolution spectra with much fine structure.

### I. INTRODUCTION

IT is well-known that the frequency response function and the unit impulse response of a linear system form a Fourier transform pair. Both functions characterize the system entirely and thus contain exactly the same information. In magnetic resonance, the frequency response function is usually called the spectrum and the unit impulse response is represented by the free induction decay. Although a spin system is not a linear system, Lowe and Norberg<sup>1</sup> have proved that under some very loose restrictions the spectrum and the free induction decay after a 90° pulse are Fourier transforms of each other. The proof can be generalized for arbitrary flip angles.<sup>2</sup>

For complicated spin systems in solution, the spectrum contains the information in a more explicit form than does the free induction decay. Hence it is generally assumed that recording the impulse response does not give any advantages compared to direct spectral techniques. The present investigations show that the impulse response method can have significant advantages, especially if the method is generalized to a series of equidistant identical pulses instead of a single pulse. In order to interpret the result, it is usually necessary to go to a spectral representation by means of a Fourier transformation. The numerical transformation can conveniently be handled by a digital computer or by an analog Fourier analyzer.

Here are some of the features of the pulse technique: (1) It is possible to obtain spectra in a much shorter time than with the conventional spectral sweep technique. The required time  $T$  for one trace is roughly given by the resolution  $\Delta$  (in cps) to be achieved,  $T \sim 1/\Delta$  sec. This allows the study of time dependent systems such as chemical reactions and transitory saturation experiments. (2) The achievable sensitivity of the pulse experiment is higher, providing the investigated spectrum possesses much

fine structure (e.g., high resolution NMR spectroscopy). All spins with resonance frequencies within a certain region are simultaneously excited, increasing the information content of the experiment appreciably compared with the spectral sweep technique where only one resonance is observed at a time. (3) The method allows the investigation of internuclear Overhauser effects. (4) The total integral and the higher moments of the spectrum can easily be determined from the initial values of the impulse response and of its derivatives, respectively. (5) The accurate frequency calibration of the spectrum is simplified and consists of an accurate time measurement.

The investigations described here employ a series of equal rf pulses equidistant in time. This is a special case of a wide band frequency source with an arbitrary, discrete or continuous power spectrum.<sup>3</sup> The optimum choice of the power spectrum depends on the purpose. The present choice has the advantages of instrumental simplicity and ease of interpretation.

Section II describes the response of a simple spin system to a series of short rf pulses. One aspect, improvement of the sensitivity, is treated here in detail. The possible enhancement is calculated in Sec. III. An experimental setup is described in Sec. IV and the results are presented in Sec. V.

### II. BEHAVIOR OF AN ISOLATED SPIN SUBJECTED TO A REPETITIVE SEQUENCE OF rf PULSES

This section describes some of the elementary features of the response of a spin system to a sequence of equally spaced, identical rf pulses. The calculations are done within the classical frame, based on the Bloch equations. Inter-correlation effects between different transitions such as Overhauser effects necessarily need a quantum mechanical theory for a satisfactory explanation.<sup>2</sup>

Suppose a system of isolated spins in a magnetic field  $H_0$

<sup>1</sup> I. J. Lowe and R. E. Norberg, *Phys. Rev.* **107**, 46 (1957); compare also A. Abragam, *The Principles of Nuclear Magnetism* (Oxford University Press, New York, 1961), p. 114.

<sup>2</sup> R. R. Ernst, "Density Operator Theory of Fourier Transform Spectroscopy" (to be published).

<sup>3</sup> The case of a "white" power spectrum is treated in R. R. Ernst and H. Primas, *Helv. Phys. Acta* **36**, 583 (1963).

along the  $z$  axis is subjected to a sequence of rectangular rf pulses along the  $x$  axis with frequency  $\omega_1$ , magnetic field amplitude  $2H_1$ , duration  $\tau$ , and period  $T$ . The system eventually reaches a stationary state, independent of the initial conditions, with a periodic motion of the magnetization.

The motion of the magnetization vector  $\mathbf{M}(t)$  is best described in a frame rotating with the frequency  $\omega_1$  around the  $z$  axis. The motion consists of two phases: (1) During the presence of the rf pulse, there is a precession around the effective field  $\mathbf{H}_{\text{leff}}$ ,

$$|\mathbf{H}_{\text{leff}}| = [(\Omega_i - \omega_1)^2 / \gamma^2 + H_1^2]^{1/2}, \quad (2.1)$$

where  $\Omega_i$  is the resonance frequency of spin  $i$  and  $\gamma$  the common gyromagnetic ratio; and (2) in the absence of the rf pulse, there is a free induction decay. For a stationary state, the initial and final positions must be identical.

If  $\gamma H_1$  is made much larger than the total width of the spectrum, it is possible to choose  $\omega_1$  such that the relation

$$(\Omega_i - \omega_1) \ll \gamma H_1 \quad (2.2)$$

is fulfilled for any line of the spectrum, so that the effective magnetic field in the rotating frame lies along the  $x$  axis and its absolute value becomes

$$|\mathbf{H}_{\text{leff}}| \sim H_1 \quad (2.3)$$

independent of the line position. If the pulse length  $\tau$  is short compared to the relaxation times  $T_1$  and  $T_2$ , relaxation is negligible during the pulse and the angle of rotation  $\alpha$ , caused by the pulse, is equal for all the nuclei,

$$\alpha = \gamma H_1 \tau. \quad (2.4)$$

The assumption that the period of the precessing magnetization is the same as the period of the pulse sequence is not necessarily true, in principle. It could happen that the magnetization returns to the original position only after  $n$  successive rf pulses or that no stationary state is reached at all. A simple algebraic analysis of the following Eqs. (2.5) and (2.6) shows that a stationary state is reached with the same periodicity as the pulse sequence if one of the side bands of the pulsed rf carrier lies in the

center of the resonance line. The same is probably also true for the off-resonance case. This is in accord with the experimental investigations.

The motion of the magnetization vector  $\mathbf{M}(t)$ , in a frame rotating with frequency  $\omega_1$ , can be represented by the following transformations as given by the Bloch equations

$$\mathbf{M}_2 = R_x(\alpha) \mathbf{M}_1 \quad (2.5)$$

and

$$\mathbf{M}_3 = R_z(\vartheta) S(T, T_1, T_2) \mathbf{M}_2 + (1 - e^{-T/T_1}) \mathbf{M}_0 = \mathbf{M}_1. \quad (2.6)$$

$\mathbf{M}_1, \mathbf{M}_2, \mathbf{M}_3$  are the positions at the beginning of the rf pulse, at the end of the rf pulse, and at the end of the free induction decay, respectively.  $R_x(\alpha)$  represents the rotation around the  $x$  axis by the angle  $\alpha$  caused by the rf pulse.  $R_z(\vartheta)$  is the operator of rotation around the  $z$  axis,  $\vartheta$  is the precession angle of the magnetization during the time  $T$  around the effective field  $(\Omega_i - \omega_1)/\gamma$  in the rotating frame,

$$\vartheta = (\Omega_i - \omega_1) \cdot T. \quad (2.7)$$

The time  $\tau$  is here neglected compared with  $T$ . The operator  $S(T, T_1, T_2)$  represents relaxation during the time  $T$  and has, in the  $(x, y, z)$  basis, the following representation,

$$S(T, T_1, T_2) = \begin{pmatrix} e^{-T/T_2} & 0 & 0 \\ 0 & e^{-T/T_2} & 0 \\ 0 & 0 & e^{-T/T_1} \end{pmatrix}. \quad (2.8)$$

$\mathbf{M}_0$  is the equilibrium magnetization which lies along the  $z$  axis. These equations allow us to calculate the  $y$  component of the magnetization,  $M_y(t)$ , which is observed in a cross coil method. Assuming that an rf pulse occurs at  $t=0$ , the  $y$  magnetization after the pulse is given by

$$M_y(t) = M_y(+0) \cos[(\Omega_i - \omega_1)t] e^{-t/T_2} + M_x(+0) \sin[(\Omega_i - \omega_1)t] e^{-t/T_2}, \quad +0 \leq t \leq T. \quad (2.9)$$

$M_y(t)$  is the  $y$  magnetization in the rotating frame. It can be measured in the laboratory frame by phase sensitive detection of the  $y$  magnetization with a reference signal in phase with the transmitter signal. The  $x$  and  $y$  components of the magnetization at the end of the rf pulse,  $M_x(+0)$  and  $M_y(+0)$ , are found to be

$$M_x(+0) = M_0 \frac{-(1 - E_1) E_2 \sin \vartheta \sin \alpha}{(1 - E_1 \cos \alpha)(1 - E_2 \cos \vartheta) - (E_1 - \cos \alpha)(E_2 - \cos \vartheta) E_2}, \quad (2.10a)$$

$$M_y(+0) = M_0 \frac{(1 - E_1)(1 - E_2 \cos \vartheta) \sin \alpha}{(1 - E_1 \cos \alpha)(1 - E_2 \cos \vartheta) - (E_1 - \cos \alpha)(E_2 - \cos \vartheta) E_2}. \quad (2.10b)$$

$E_1$  and  $E_2$  are abbreviations for the exponentials  $e^{-T/T_1}$  and  $e^{-T/T_2}$ . Equation (2.9) shows that the phases of the oscillations after each pulse depend on the frequency

deviation  $\Omega_i - \omega_1$ . The phase differs thus from line to line within the same spectrum. The deviation depends on the pulse spacing  $T$ . If  $T$  is much longer than the relaxation

time  $T_1$ , the response of each pulse is independent of the preceding pulses and the initial magnetization reduces to

$$M_x(+0)=0, \quad M_y(+0)=M_0 \sin\alpha. \quad (2.11)$$

In applying the pulse technique to enhance the sensitivity (Sec. III), it is important to determine the optimum performance conditions for maximum signal. The magnetization depends on two free parameters, the pulse spacing  $T$  and the flip angle  $\alpha$ . The pulse spacing is usually fixed by the necessary frequency range and by resolution requirements (as discussed in Sec. III). Both components,  $M_x(+0)$  and  $M_y(+0)$ , depend in the same manner on the flip angle  $\alpha$ . The optimum angle for producing the maximum magnetization in the  $x$ - $y$  plane is easily found to be

$$\cos\alpha_{\text{opt}} = \frac{E_1 + E_2(\cos\vartheta - E_2)/(1 - E_2 \cos\vartheta)}{1 + E_1 E_2(\cos\vartheta - E_2)/(1 - E_2 \cos\vartheta)}. \quad (2.12)$$

For  $T \gg T_1$  the optimum flip angle approaches  $90^\circ$ , which is the optimum flip angle for a single pulse experiment. For sufficiently short pulse spacings,  $T \ll T_2$ , the average rf amplitude  $(\gamma H_1)_{\text{opt}}(\tau/T) = \alpha_{\text{opt}}/T$  can be shown to

$$C_n = M_0 \frac{T_2}{(\Delta\omega T_2)^2 + 1} \frac{1}{(2T)^\dagger} \frac{(1 - E_1)(1 - 2E_2 \cos\vartheta + E_2^2) \sin\alpha}{(1 - E_1 \cos\alpha)(1 - E_2 \cos\vartheta) - (E_1 - \cos\alpha)(E_2 - \cos\vartheta)E_2}, \quad (2.15)$$

with  $\Delta\omega = \Omega_i - \omega_1 - 2\pi(n/T)$ , and where the term containing  $\Delta\omega' = \Omega_i - \omega_1 + 2\pi(n/T)$  has been neglected.

This expression shows the interesting fact that the resulting line shape is identical to the line shape observed in a slow pass, low power spectral experiment. The line shape is independent of  $T$ ,  $\alpha$ , and  $\vartheta$ . Since it is also independent of the applied rf power no line broadening occurs in contrast to the conventional slow passage saturation experiments. However, the line intensities depend in a complicated manner on all three parameters.

The manner in which the line depends on these three parameters as well as on the relaxation times  $T_1$  and  $T_2$  is discussed for optimum flip angle  $\alpha_{\text{opt av}}$  [Eq. (2.14)]. The Fourier coefficients in this case are given by

$$C_n = M_0 \frac{T_2}{(\Delta\omega T_2)^2 + 1} \frac{1}{(2T)^\dagger} \left( \frac{1 - E_1}{1 + E_1} \right)^\dagger \times \left( 1 + E_2 \frac{E_2 - \cos\vartheta}{1 - E_2 \cos\vartheta} \right). \quad (2.16)$$

The dependence of the signal intensity on  $\vartheta$  can cause inaccurate measurements of relative line intensity. The maximum variation of the intensities is given by the ratio of maximum to minimum Fourier coefficient  $C_n$  as a

function of  $\vartheta$ ,

$$[(\gamma H_1)_{\text{opt}}(\tau/T)]^2 T_1 T_2 = 1, \quad (2.13)$$

providing one of the pulse side bands coincides with the center of the resonance line. The optimum flip angle depends on the precession angle  $\vartheta$  which varies from line to line within the same spectrum. An average optimum flip angle  $\alpha_{\text{opt av}}$ , independent of  $\vartheta$ , is given by

$$\cos\alpha_{\text{opt av}} = E_1. \quad (2.14)$$

The Fourier transform of the response to a sequence of rf pulses, given by Eq. (2.9), now is determined. As long as the pulse spacing  $T$  is much longer than  $T_1$ , the Fourier transform is identical with the spectrum of the spin system, according to Ref. (1). The Fourier cosine transform yields the absorption mode spectrum, and the Fourier sine transform yields the dispersion mode spectrum. If the pulse spacing is comparable with  $T_1$ , distortions occur in the spectrum. The Fourier transform of a periodic signal with period  $T$  is, of course, a discrete spectrum with the frequencies  $f = n/T$  ( $n = 0, 1, 2, \dots$ ). The corresponding coefficients  $C_n$  of the Fourier cosine transform of the free induction decay [Eq. (2.9)] are given by<sup>4</sup>

function of  $\vartheta$ ,

$$[C_n(\vartheta)_{\text{max}}/C_n(\vartheta)_{\text{min}}]_{\alpha_{\text{opt av}}} = (1 + E_2)/(1 - E_2). \quad (2.17)$$

This variation is negligible for a sufficiently long pulse spacing ( $T/T_2 = 3$  causes a maximum variation of  $\pm 5\%$ ). The dependence of the intensity on  $T_2$  is also negligible if  $e^{-T/T_2} \ll 1$ . The dependence on  $T_1$  can be important if  $T_1$  is much longer than  $T_2$  and if  $T_1$  varies strongly from line to line within the same spectrum. This problem occurs in a similar manner in slow passage experiments if the rf power is optimized for maximum intensities. The influence of  $T_1$  on the intensities is small if  $e^{-T/T_1} \ll 1$  (for  $T/T_1 \geq 3$ , the influence is less than  $\pm 2.5\%$ ).

The true free induction decay after a single rf pulse extends, in principle, to infinity and the corresponding Fourier transform is a continuous spectrum. Since the

<sup>4</sup> The Fourier coefficients are calculated by means of the formula  $C_n = (2/T)^\dagger \int_0^T \cos(2\pi nt/T) M_y(t) dt$   
 $= (2T)^\dagger (1/c) \sum_{k=0}^{c-1} \cos(2\pi kn/c) M_y(Tk/c) \quad (n = 1, 2, \dots)$ .

The last equality holds if  $M_y(t)$  does not contain frequencies higher than  $c/2T$ , where  $c$  is the number of samples within the time  $T$ . This is a consequence of the sampling theorem. The factor  $2/T$  is chosen such that

$$\int_0^T M_y^2(t) dt = \sum C_n^2 + S_n^2,$$

where  $S_n$  are the corresponding Fourier sine coefficients.

impulse response, given by Eq. (2.9), is defined only in the time interval  $0-T$ , the Fourier spectrum consists of discrete lines with a spacing of  $1/T$  cps. The values approximately represent discrete points of the true spectrum.

To obtain a continuous spectrum it is necessary to make assumptions about the impulse response for  $t > T$ . Under the usual experimental conditions, the free induction decay signal is small for  $t > T$ . It is reasonable to assume that the impulse response can be set equal to zero for  $t > T$ ,

$$M_y(t) = 0, \quad t > T. \quad (2.9a)$$

$$C(\omega) = M_0 \frac{1}{(2T)^{\frac{1}{2}} (1-E_1 \cos\alpha)(1-E_2 \cos\vartheta) - (E_1 - \cos\alpha)(E_2 - \cos\vartheta)E_2} \times \left\{ \left\{ \frac{T_2}{[(\Delta\omega T_2)^2 + 1]} \right\} \left\{ 1 - E_2 [\cos\vartheta + \cos(\Delta\omega T)] + E_2^2 \cos(\omega T) \right\} + \left\{ \frac{\Delta\omega T_2^2}{[(\Delta\omega T_2)^2 + 1]} \right\} [\sin(\Delta\omega T) - \sin\vartheta + E_2 \sin(\omega T)] E_2 \right\} \quad (2.18)$$

with  $\Delta\omega = \Omega_i - \omega_1 - \omega$ . This formula reduces to Eq. (2.15) for  $\omega = 2\pi n/T$ . The spectrum consists of absorptive and dispersive parts whose relative coefficients are of the order 1 and  $E_2$ , respectively. The dispersive part affects chiefly the wings and can be neglected if  $e^{-T/T_2} \ll 1$ . The maximum variation of the absorptive part as a function of  $\vartheta$  is again given by Eq. (2.17), for the flip angle  $\alpha_{opt}$  determined by Eq. (2.14). Here not only the intensities but also the line shape is affected.

It is possible to improve the resolution, given so far by the spacing  $1/T$  of the Fourier coefficients [Eq. (2.15)], by calculating some additional points of the continuous spectrum [Eq. (2.18)]. However when the inherent error, expressed by Eq. (2.18), becomes larger than the intensity difference between two adjacent points there is no advantage in calculating further intermediate points.

### III. APPLICATION FOR SENSITIVITY IMPROVEMENT

The main stimulus to investigate this pulse method was the expected increase in sensitivity, which makes the method of interest to chemists and biologists.

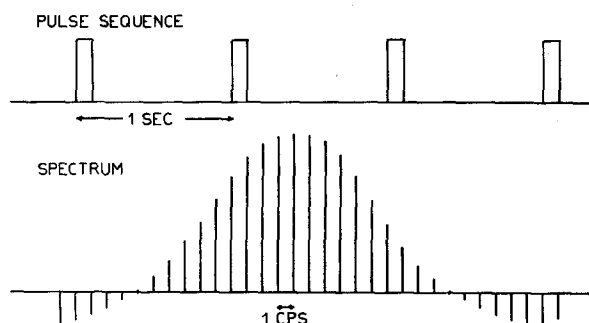


FIG. 1. Example of a repetitive pulse sequence and the corresponding frequency spectrum as a method to generate a multifrequency source.

The Fourier transformation of  $M_y(t)$ , given by Eqs. (2.9) and (2.9a), produces a continuous spectrum. The accuracy of the points of the continuous spectrum which lie between the values given by Eq. (2.15) is somewhat less than the accuracy of the harmonics of  $1/T$ . The accuracy again depends on the ratio  $T/T_2$  and is improved by making  $T$  large.

The Fourier cosine transform, corresponding to the absorption spectrum, now has the form

To make the possible enhancement of the sensitivity intuitively clear, it is helpful to consider the problem from another viewpoint. The conventional spectral methods in magnetic resonance use a field or frequency sweep to record a spectrum. At any particular time, the transmitter frequency corresponds to one single point in the spectrum and the rest of the spectrum is for the most part disregarded. This corresponds in optical spectroscopy to a very narrow slit through which the spectrum is observed. It is obvious that the information rate of such an experiment could be greatly increased by investigating the entire spectrum during the total available time. This could be done, at least in principle, by using several transmitters and receivers with different frequencies which correspond to different points in the spectrum. This kind of spectrometer could be called a multichannel spectrometer. The sensitivity improvement which is achievable depends on the total number of channels.

Applying a sequence of equally spaced short rf pulses corresponds to a multichannel experiment. This becomes clear by considering the frequency spectrum of an rf pulse sequence with the pulse length  $\tau$  and the pulse spacing  $T$ . It consists of numerous side bands of the carrier frequency  $\omega_1$ ,  $1/T$  cps apart. The Fourier coefficients of the frequencies  $f_n = \omega_1/2\pi + n/T$  are given by

$$A_n = [\sin(n\pi\tau/T)] / (n\pi\tau/T) \quad (3.1)$$

(see Fig. 1). To obtain a side band spectrum of constant amplitude throughout  $F$ , the width of the spectrum being investigated, it is necessary that

$$\pi F\tau \ll 1. \quad (3.2)$$

The resolution and the faithful representation of the spectrum are determined by the density of these side band frequencies; e.g., by the spacing  $T$  of the pulses.

Each side band produces a response which is determined by the value of the spectrum at its frequency. The amplitudes of these responses can be determined by a Fourier analysis and allow the spectrum to be determined. This treatment can be used only for very crude qualitative arguments because of the nonlinearity of the spin system. The influence of the different frequency components of the pulse sequence cannot be considered separately unless the inequality

$$\gamma H_1 \tau \ll 1 \quad (3.3)$$

is satisfied. If this inequality does not hold, the treatment of Sec. II must be used.

To obtain an improvement in sensitivity it is essential that the responses after each pulse are added together coherently. This can conveniently be done by using a time averaging computer. The final step is then the Fourier transformation of the time averaged free induction decay. The Fourier analysis is equivalent to using a multichannel receiver.

In order to show the possible improvement of the signal-to-noise ratio obtainable with the pulse method, it is useful to compare the pulse method with a single scan, slow passage experiment done in the same time  $T_i$ . It is assumed that the noise has a white power spectrum with the power density  $P$  in  $W/(\text{cps})$ . The total sweep width to be covered is denoted by  $F$  (cps). The signal-to-noise ratio  $S/N$  is defined here as the ratio between the peak signal amplitude and the rms noise amplitude.

The  $S/N$  ratio of the single scan experiment is calculated first. It is of advantage to use a linear filter at the output of the spectrometer to limit the noise bandwidth. The theoretically optimum filter delivering the maximum available  $S/N$  ratio is the matched filter.<sup>5</sup> Its shape depends on the line shape to be filtered. One can show that the maximum available  $S/N$  ratio is given by

$$\left(\frac{S}{N}\right)^2 = \frac{1}{RP} \int_{-\infty}^{\infty} v(t)^2 dt, \quad (3.4)$$

where  $R$  is the resistance over which the voltages are measured and  $v(t)$  is the absorption mode signal in question. It is known<sup>6</sup> that in a true slow passage experiment the maximum  $S/N$  ratio is achieved for a saturation parameter  $S = (\gamma H_1)^2 T_1 T_2 = 2$ . The absorption mode signal  $v(t)$  is in this case given by

$$v(t) = M_0 \left(\frac{T_2}{T_1}\right)^{\frac{1}{2}} \frac{\sqrt{2}}{3 + (2\pi a t)^2 T_2^2}.$$

The sweep rate  $a$ , in cps/sec, can be expressed by the total

available time  $T_i$  and the sweep range  $F$ ,  $a = F/T_i$ . If one inserts this expression into Eq. (3.4), one obtains for the  $S/N$  ratio of a single scan

$$(S/N)_s^2 = (1/6\sqrt{3})(M_0^2/RP)(T_i/T_1 \cdot F). \quad (3.5)$$

In most spectrometers, a modulation method is used for baseline stabilization. It delivers a somewhat smaller  $S/N$  ratio.<sup>7</sup> Assuming a centerband method, the above calculated  $S/N$  ratio has to be corrected by the factor  $1.14/\sqrt{2}$ ,

$$(S/N)_c^2 = (1.30/12\sqrt{3})(M_0^2/RP)(T_i/T_1 \cdot F). \quad (3.6)$$

The  $S/N$  ratio of the corresponding pulse experiment, performed in the same total time  $T_i$  by recording and summing all the responses to  $n$  rf pulses, is given by

$$(S/N)_p^2 = (n \cdot s_{\max})^2 / (RPBT_i/2). \quad (3.7)$$

Here,  $s_{\max}$  is the maximum Fourier component of a single impulse response,  $n \cdot s_{\max}$  is the total accumulated signal height and corresponds to  $v_{\max}$  in the single scan experiment.  $PBT_i/2$  is the total noise energy accumulated during the time  $T_i$  with the effective bandwidth  $B$  of a single Fourier component. The equidistant Fourier components with the frequencies  $f = m/T$ , where  $T = T_i/n$  is the pulse spacing, have the effective bandwidth  $B$ ,

$$B = 2/T. \quad (3.8)$$

The factor 2 in Eq. (3.7) occurs because the Fourier cosine transformation [Eq. (2.15)] halves the noise power by selecting only one phase. The factor 2 in Eq. (3.8) occurs because both of the sidebands,  $\omega_1/2\pi + f$  and  $\omega_1/2\pi - f$ , contribute to the noise at the frequency  $f$  after demodulation. Equation (3.8) assumes the existence of a band limiting low pass filter at the frequency  $F$  (as explained in Sec. IV) which prevents the down conversion of high frequency noise in the digitizing process.

The noise in the Fourier spectrum is the Fourier transform of the original noise at the output of the spectrometer. In general, it can change its character entirely by the Fourier transformation. Stationary nonwhite noise becomes nonstationary, whereas stationary white noise remains stationary and white after the Fourier transformation.

To achieve the maximum possible  $S/N$  ratio with the pulse technique, it is again necessary to use a matched filter, determined by the line shape. However, in the present case the filter is readily achieved. The filtering process corresponds to a convolution integral between the spectrum and the filter impulse response. In the Fourier time domain, this corresponds to multiplication of the free induction decay with the frequency response function which is a trivial process for the computer to perform. In the case of Lorentzian lines with a common relaxation

<sup>5</sup> S. Goldman, *Information Theory* (Prentice-Hall, Inc., Englewood Cliffs, New Jersey, 1953), p. 230; and L. S. Schwartz, *Principles of Coding, Filtering and Information Theory* (Spartan Books, Inc., Baltimore, 1963), p. 136.

<sup>6</sup> R. R. Ernst and W. A. Anderson, *Rev. Sci. Instr.* **36**, 1696 (1965).

<sup>7</sup> W. A. Anderson, *Rev. Sci. Instr.* **33**, 1160 (1962).

time  $T_2$ , the envelope of the decay is given by  $e^{-t/T_2}$ . Since the  $S/N$  ratio is proportional to the envelope height, it is obvious that it deteriorates towards the end of the trace. It is intuitively clear that the best  $S/N$  ratio after the Fourier transformation is obtained by weighting each point of the free induction decay with its own  $S/N$  ratio. For a Lorentzian line this results in multiplication of the trace by  $e^{-t/T_2}$ . It can be proved rigorously that this is exactly equivalent to the use of a matched filter.

To determine the maximum Fourier component  $s_{\max}$  of Eq. (3.7), the  $y$  component of the free induction decay [Eq. (2.9)] must be multiplied by the matched filter function  $e^{-t/T_2}$  and then Fourier transformed,

$$s_{\max} = \left(\frac{2}{T}\right)^{\frac{1}{2}} \int_0^T \cos\left(2\pi n \frac{t}{T}\right) M_y(t) e^{-t/T_2} dt \\ = M_y(+0) \frac{1}{(2T)^{\frac{1}{2}}} \frac{T_2}{2} (1 - E_2^2). \quad (3.9)$$

It is assumed here that one of the pulse modulation side bands lies exactly on resonance  $\Omega_1 - \omega_1 = 2\pi n/T$ . This gives  $\cos\theta = 1$ . In this case  $M_x(+0)$  disappears and the magnetization  $M_y(t)$  is determined alone by  $M_y(+0)$ , Eq. (2.10). Deviations from this assumption can easily be included by using the results of Sec. II. The initial magnetization  $M_y(+0)$  is calculated for the optimum flip angle  $\alpha_{\text{opt}}$  which is given in Eq. (2.12).

The action of the matched filter on the noise is essentially a uniform attenuation of all noise frequencies. The power spectrum remains unchanged providing it is a sufficiently smooth function of frequency. The power density  $P$  of the white noise is changed to  $P_f$  according to

$$P_f = P \cdot \frac{1}{T} \int_0^T e^{-2t/T_2} dt = P \cdot \frac{T_2}{2T} (1 - E_2^2). \quad (3.10)$$

Inserting Eqs. (3.8)–(3.10) into Eq. (3.7), the maximum  $S/N$  ratio of the pulse experiment becomes

$$\left(\frac{S}{N}\right)_p = \frac{nT_2}{4RP} M_0^2 \frac{(1 - E_1)^2}{1 - E_1^2}. \quad (3.11)$$

The ratio of the sensitivities of the pulse experiment and of the steady state experiment performed in the same total time can be found after slight rearrangements to be

$$\frac{(S/N)_p}{(S/N)_s} = 0.799 \left(\frac{F}{\Delta}\right)^{\frac{1}{2}} G\left(\frac{T}{T_1}\right),$$

with

$$G(x) = \left[ \frac{1}{2} \frac{(1 - e^{-x})^2}{x(1 - e^{-2x})} \right]^{\frac{1}{2}}. \quad (3.12)$$

The function  $G(T/T_1)$  is displayed in Fig. 2. It varies slowly and can often be approximated by one. The possible

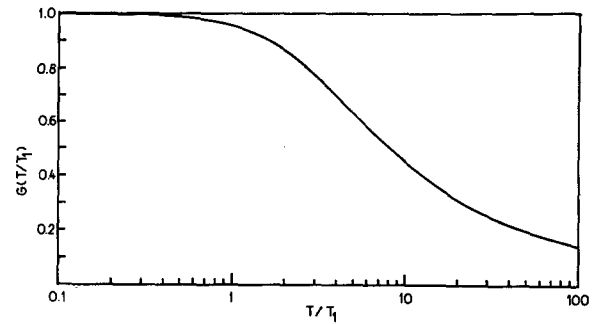


FIG. 2.  $S/N$  improvement by means of the pulse method, dependence on the ratio of pulse spacing  $T$  to relaxation time  $T_1$ , represented by the function  $G(T/T_1)$  which is given by Eq. (3.12).

gain in sensitivity is thus essentially given by the ratios of the total sweep width  $F$  to a characteristic line width  $\Delta = 1/\pi T_2$ . This is a plausible result which shows that the gain is equal to the square root of the total available time to the time actually spent within a single line of the width  $\Delta$  using the ordinary spectral sweep technique. The time actually saved in achieving a certain  $S/N$  ratio is roughly the ratio of total sweep width to a characteristic linewidth. A factor of 100 in time can be gained easily.

Some important facts in connection with Eq. (3.12) have to be remembered:

(1) *Sweep width  $F$ .* In favorable cases, the sweep rate  $F$  is identical with the width of the investigated spectrum. Often, the width of the spectrum is not known in advance and can not be determined easily. Here,  $F$  is more likely the maximum range of possible chemical shift values.

(2) *Choice of the pulse spacing  $T$ .* According to Eq. (3.12), the gain in  $S/N$  ratio increases slightly by using a shorter pulse spacing. However, there are factors which limit the minimum useful pulse spacing. In Sec. II, it was shown that the longer  $T$  is, the better the calculated points represent actual points of the spectrum. The optimum choice depends on the relative emphasis with respect to resolution and to sensitivity. In addition, in many experiments the pulse spacing is determined by the sweep range  $F$  necessary to cover the entire spectrum and by the number of channels  $c$  of the digital storage used to add the impulse responses together. (With this method it is impossible only to analyze a fraction of a spectrum.) The total spectrum has to lie on one side of the carrier frequency  $\omega_1$  and within  $\omega_1 \pm f_{\max}$ , where  $f_{\max} = c/2T$  is the maximum frequency component which can be analyzed with  $c$  samples within the time  $T$ . This requires that the pulse spacing be equal to or shorter than  $T_{\max} = c/2F$ .

(3) *Deviations from the slow passage conditions.* This comparison was based on a true slow passage experiment. It is well-known that intermediate passage

conditions allow considerable improvement in the  $S/N$  ratio.<sup>6</sup> This is more pronounced for larger ratios of  $T_1/T_2$ . By comparing the pulse experiment with an intermediate passage experiment the actual gain is smaller. Thus, the pulse method may not be as useful for improving the sensitivity in systems with very high  $T_1/T_2$  ratios. But it has the advantage that it gives no appreciable line deformations as they occur in intermediate or rapid passage experiments.

(4) *Line broadening.* The use of an optimum saturation parameter  $S=2$  in slow passage experiments produces a line broadening by a factor  $\sqrt{3}$ . The pulse experiment described here does not show any line broadening, irrespective of the applied rf field strength. The inherent resolution of this experiment is therefore somewhat higher.

#### IV. EXPERIMENTAL

This section describes an experimental arrangement which was successfully used to enhance the sensitivity of proton magnetic resonance spectra using a Varian Associates double purpose 60 Mc spectrometer DP60. A block diagram of the modified spectrometer is shown in Fig. 3. The pulsed 60 Mc transmitter frequency is generated by pulsing a 30 Mc carrier and afterwards doubling the frequency to eliminate any 60 Mc leakage.<sup>8</sup> The 30 Mc signal is taken from the transmitter unit V4311 and fed into a pulse gate consisting of two gate stages, frequency doubler, and power amplifiers, which deliver a peak power of 200 W into a load of 100  $\Omega$ . A typical pulse length is  $\tau=100 \mu\text{sec}$ . The pulse spacing  $T$  is typically 0.5–2 sec and the peak-to-peak rf voltage 50–250 V.

The rf pulses are fed into the transmitter coil of the cross coil arrangement of the high resolution NMR probe. The induced signal in the receiver coil is fed to the receiver, where it is amplified, converted to 5 Mc, and demodulated in a phase sensitive detector. The existing phase sensitive detector of the V4311 unit is changed to have a passband of 5 kc. The free induction decay, containing frequencies up to 500 cps, is fed into the time averaging computer C1024 (Varian Associates) where the signal is digitized in 1024 sample points, equidistant in time, and added to the values already stored.

The highest frequency which can be retrieved from the computer is  $c/2T$  cps,  $c$  is the number of channels ( $c=1024$ ) and  $T$  is the pulse spacing. If higher frequencies are fed in, they are down converted into the frequency range  $0 \rightarrow c/2T$  and appear in the output as lower frequencies  $f' = |f - nc/T|$  ( $n=0, 1, 2, \dots$ ). To avoid possible false resonances originating from this, the impulse response should not contain frequencies higher than  $F=c/2T$ . In

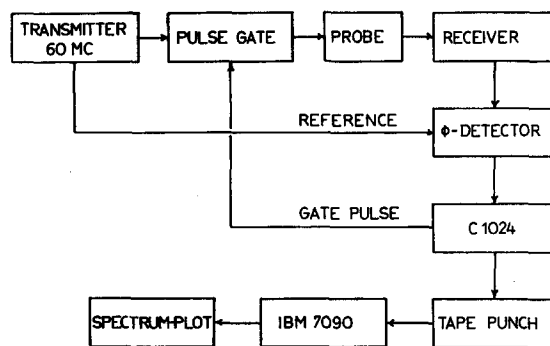


Fig. 3. Instrumental arrangement to record and Fourier transform the impulse response, using a modified Varian DP60.

addition, noise at frequencies above  $F$  is down converted in the frequency range below  $F$  and increases the power density of the noise in the critical range. Thus, it is important that the bandpass is limited before sampling in the time averaging computer.

The necessary low pass filter with a 3 dB point in the region of  $F$  introduces an undesirable frequency dependent phase shift into the passband. This complicates the selection of the true absorption mode signal during the Fourier transformation. To minimize the phase shift, a simple RC filter is used in front of the sampling device with a time constant of  $RC \sim 1/2\pi F$ .

To accumulate the impulse response, the time averaging computer is driven in the repetitive mode using the internal trigger. The same trigger pulse is used to open the transmitter gate for 100  $\mu\text{sec}$  at the beginning of each trace to generate the rf pulse. After a sufficient number of scans, the accumulated signal in the memory of the C1024 is read out through the data output unit model 220 C<sup>9</sup> which converts the binary code into bcd numbers. They are punched on paper tape using a perforator model 420.<sup>10</sup> The punched tape is used as the input for an IBM 7090 digital computer which calculates the Fourier transform of the impulse response and plots the spectrum automatically by means of an incremental curve plotter.

#### Computer Program for the Fourier Transformation

A simplified block diagram of the computer program is shown in Fig. 4. Only the 512 ( $=c/2$ ) Fourier components corresponding to harmonics of the fundamental frequency  $1/T$  were calculated.

The adjustment of the phase to get a pure absorption mode signal can cause severe difficulties. The first correction to be made concerns the phase shift introduced by the band limiting filter mentioned above. The total phase shift and attenuation of this filter and the receiver were measured as a function of the frequency. The computer separately calculates the sine and cosine transform of the

<sup>8</sup> S. Meiboom and D. Gill, Rev. Sci. Instr. 29, 688 (1958).

<sup>9</sup> Technical Measurement Corporation (North Haven, Connecticut).

<sup>10</sup> Tally Corporation (Seattle, Washington).

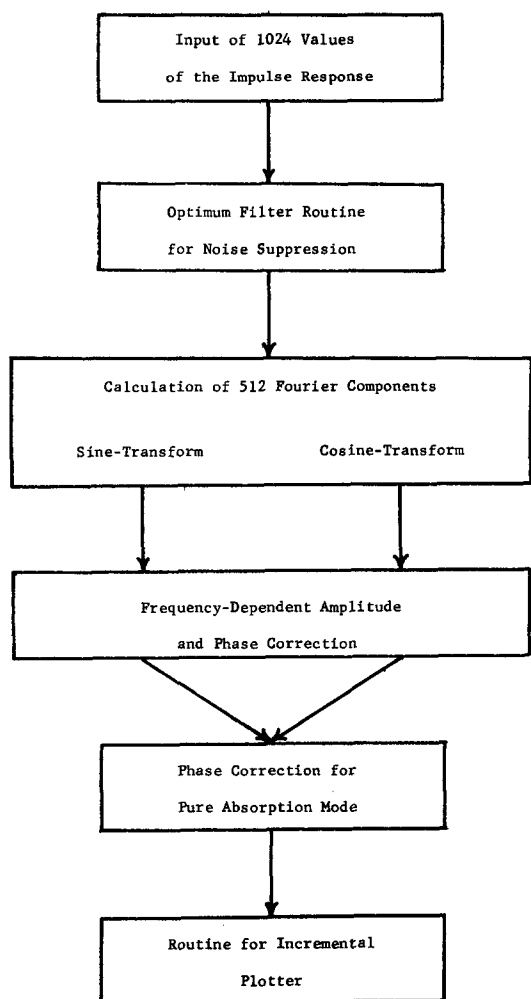


FIG. 4. Simplified block diagram of the computer program for the Fourier transformation.

impulse and then combines them to obtain a spectrum with frequency independent phase.

It is not practical to adjust manually the phase of the 5 Mc phase sensitive detector to obtain a pure absorption

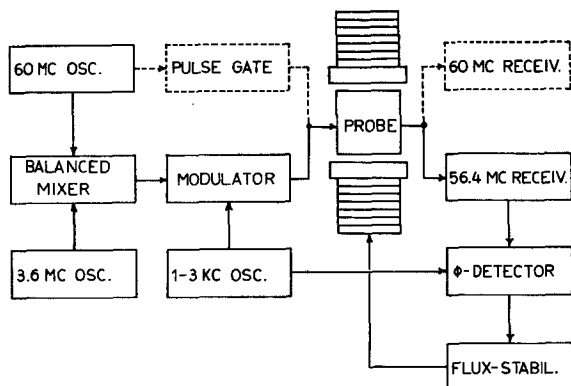


FIG. 5. Instrumental arrangement for the stabilization of the magnetic field in proton resonance. The magnetic field is locked on an internal fluorine reference signal.

mode signal. Consequently, one usually obtains a mixture of absorption and dispersion modes. However, it is easy to include a routine in the computer program to correct the phase. For this purpose the computer calculates the Fourier cosine transform  $s_c(\omega)$  and the Fourier sine transform  $s_s(\omega)$  of the impulse response. The true absorption mode signal  $s_a(\omega)$  is then given by

$$s_a(\omega) = s_c(\omega) \cos \varphi + s_s(\omega) \sin \varphi.$$

The correct angle  $\varphi$  of the phase adjustment is determined by the computer by maximizing the ratio  $R(\varphi) = A_u(\varphi)/A_l(\varphi)$  as a function of the phase  $\varphi$ .  $A_u(\varphi)$  and  $A_l(\varphi)$  are the areas above and below the corrected signal trace  $s_a(\omega)$  limited by the maximum and the mini-

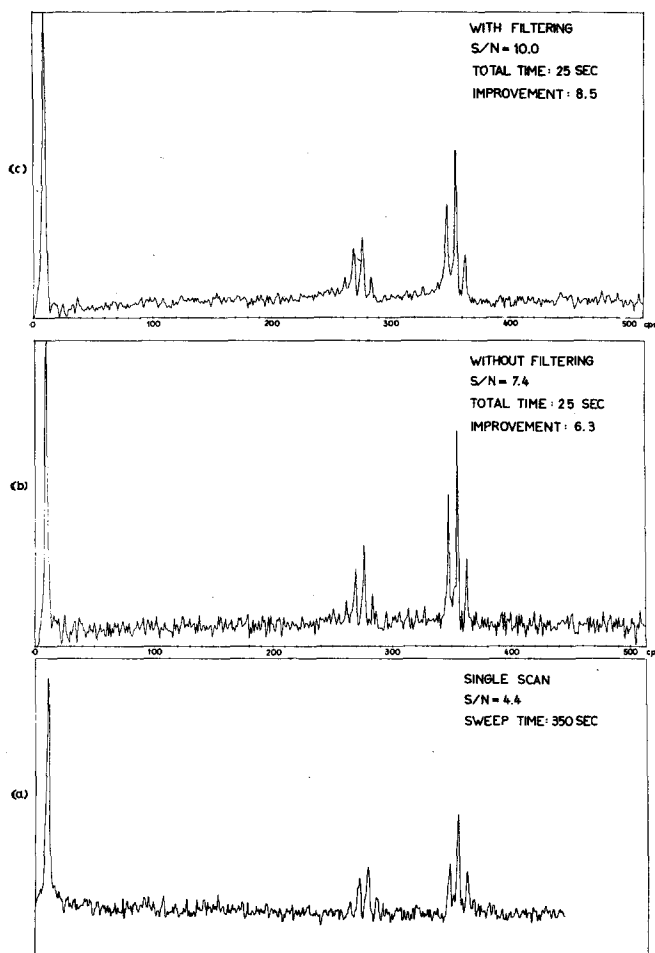


FIG. 6. Three spectra of 1% ethylbenzene dissolved in hexafluorobenzene. [The  $S/N$  ratio is indicated for the strongest line of the quartet, using the customary practical definition:  $S/N = 2.5 \times \text{peak value of the signal} / \text{peak-to-peak value of the noise}$ .] (a) Single scan, the absorption mode signal is directly recorded in 350 sec. (b) Pulse method, applying 25 pulses, 1 sec apart and adding the 25 responses together. The spectrum is obtained by means of a Fourier transformation. 512 points with 1 cps distance are calculated and plotted. The zero point marks the position of the 60 Mc carrier frequency. (c) Same spectrum as in (b), using a filtering procedure in the computer calculation to suppress the noise.



mum, respectively, of  $s_a(\omega)$  and are given by

$$A_u(\varphi) = \sum_k [s_{a \max} - s_a(2\pi k/T)],$$

$$A_l(\varphi) = \sum_k [s_a(2\pi k/T) - s_{a \min}].$$

This method is independent of the actual line shape. It gives the correct phase angle for pure absorption mode if the  $S/N$  ratio is sufficiently high. The sensitivity of this method is higher for a wide sweep width.

#### Field-Frequency Stability

For coherent summation of different traces of the same impulse response, it is necessary to maintain high field-frequency stability for the total time  $T_t$ . The variations must be small compared to the line width of the observed spectrum. In the case of high resolution proton magnetic resonance, stability of  $\pm 0.1$  cps is necessary. This is usually achieved by means of an internal field-frequency lock,<sup>11</sup> which locks the field on the dispersion mode signal of a reference line in the analytical sample. Because the spectrum to be investigated is covered with side bands due to the pulsing, it is of advantage to stabilize on the resonance of a different nuclear species. In the present experiments, investigating proton resonance, the field is locked on a strong fluorine resonance by using a fluorine-containing, proton-free compound as solvent. A convenient solvent was found to be hexafluorobenzene.<sup>12</sup> The instrumentation is sketched in Fig. 5. The transmitter frequency for fluorine resonance is generated by mixing the proton transmitter frequency of 60 Mc with a stable, quartz controlled frequency of 3.6 Mc in a balanced

mixer, suppressing the carrier frequency. To be able to position the 60 Mc carrier anywhere with respect to the proton spectrum, the fluorine signal is locked on an audio side band of the 56.4 Mc carrier. The modulation frequency of 1.5–3 kc is detected in a phase sensitive detector and the dispersion mode signal is used to correct the magnetic field. The audiofrequency is adjusted so that the 60 Mc carrier is just outside of the total range of the proton spectrum. (All the lines have to lie on one side of the carrier because after phase sensitive demodulation of the signal by means of the transmitter frequency it is not possible to distinguish negative from positive frequencies.)

Transmitter and receiver coils are used in common for both frequencies, 60 and 56.4 Mc, and both are tuned to 60 Mc to give a good  $S/N$  ratio for proton spectra. The  $S/N$  ratio of the fluorine resonance is poor and a strong reference line is necessary.

#### V. RESULTS

To test the theoretical result of Sec. III, spectra were recorded using both the pulse technique and conventional spectral recording. All the experiments were done on the same spectrometer with the same rf units to make sure that the inherent instrumental sensitivity was constant. (No attempts were made to optimize the common parts of both experiments such as the preamplifier, etc., since these do not affect the ratios of the sensitivities.) The single section RC filter used in the conventional spectrometer and the rf power in both experiments were adjusted empirically to give the best  $S/N$  ratios.

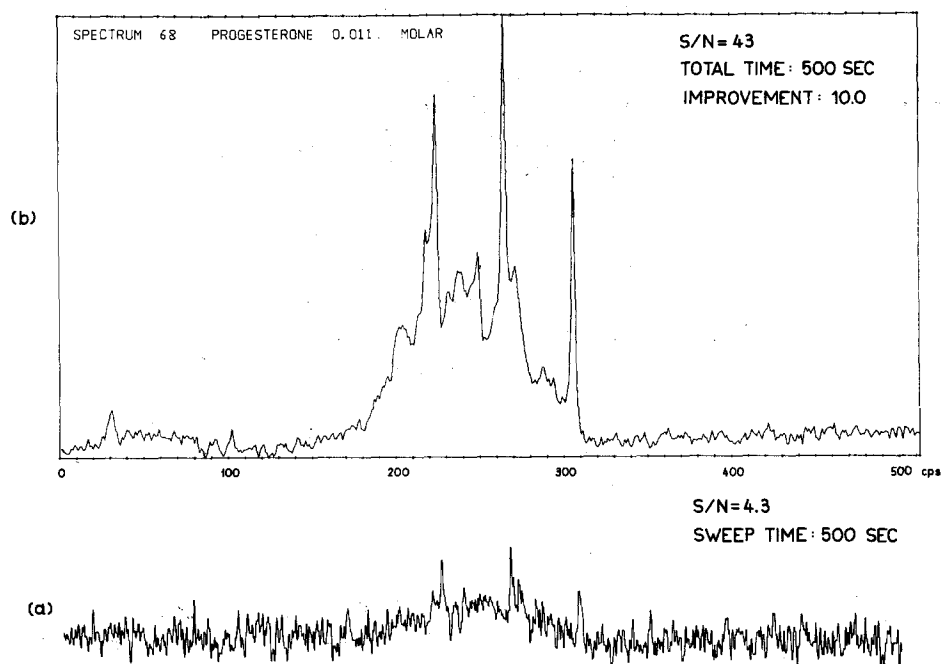


FIG. 7. Two spectra of a 0.011 *M* solution of progesterone in hexafluorobenzene, both spectra performed in 500 sec. [The  $S/N$  ratio is indicated for the strongest line of the spectrum, using the customary practical definition:  $S/N = 2.5 \times$  peak value of the signal/peak-to-peak value of the noise.] (a) Single scan, the absorption mode signal is recorded directly. (b) Pulse method, applying 500 pulses, 1 sec apart and adding the 500 responses together. The spectrum is obtained by means of a Fourier transformation. 512 points with 1 cps distance are calculated and plotted. The zero point marks the position of the 60 Mc carrier frequency.

<sup>11</sup> W. A. Anderson (unpublished work); and H. Primas, 5th European Congr. Mol. Spectry. (June 1961).

<sup>12</sup> City Chemical Corporation (New York).

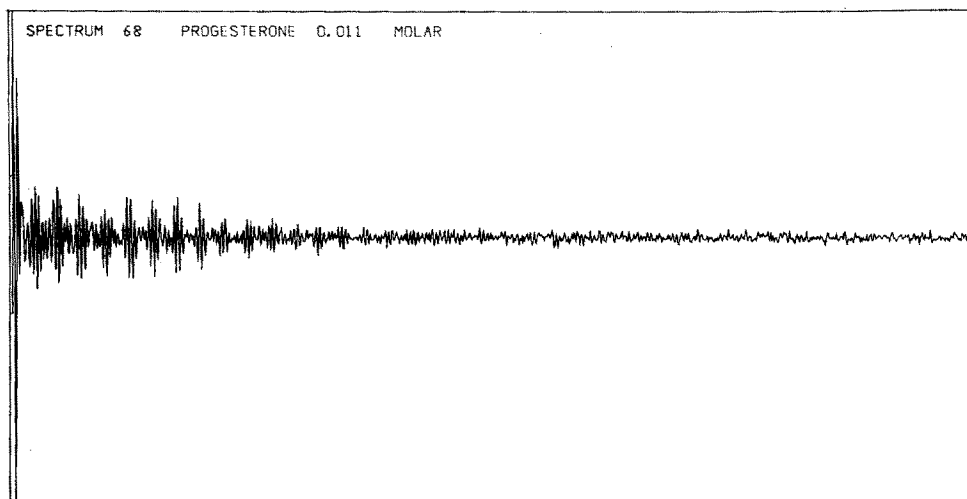


FIG. 8. Impulse response of a 0.011 *M* solution of progesterone in hexafluorobenzene. It consists of the sum of 500 traces, each trace of 1 sec length. The Fourier transform of this impulse response is shown in Fig. 7 (b).

The sweep range was chosen to be 512 cps. This corresponds closely to the sweep range used in routine measurements of proton resonance spectra at 60 Mc. It is usually necessary to use a sweep range considerably wider than the width of the investigated spectrum because of the uncertainty of the accurate line positions.

Figure 6 shows three spectra of a solution of 1% ethylbenzene in hexafluorobenzene. The lowest trace corresponds to a single scan in 350 sec for a sweep range of 512 cps. The middle trace was taken with the pulse technique and results from 25 pulses spaced 1 sec apart. Filtering was not included in the computer routine. The improvement of the *S/N* ratio, considering the shorter performance time, is 6.3. The *S/N* ratio can further be improved, as shown in the top trace, by using a filter procedure in the computer program. The total observed improvement in *S/N* is a factor 8.5. The theoretical improvement, assuming a line width of 2 cps for the quartet should be  $0.799 \times (512/2)^{1/2} = 12.8$ . The slight discrepancy is probably due to the deviation from the true slow passage conditions in the single scan experiment.

Figure 7 compares two spectra of a 0.011 *M* solution of progesterone in hexafluorobenzene taken with the two methods, single sweep and pulse method, using the same total time of 500 sec. The observed improvement is a factor 10.0 and corresponds closely to the theoretically expected value. The peak on the left side of the spectrum in Fig. 7 is caused by the single proton at the double bond of progesterone. The corresponding impulse response used to calculate the spectrum in Fig. 7 is displayed in Fig. 8.

## VI. DISCUSSION

The theoretical results of Sec. III and the experimental results of Sec. V show that Fourier transform spectroscopy is able to improve the sensitivity of magnetic resonance experiments effectively if certain conditions are fulfilled which can be summarized as follows:

- (1) The longitudinal relaxation time  $T_1$  must not be too long compared with  $T_2$ . Otherwise, it is possible to gain about the same improvement by an intermediate passage experiment, combined with time averaging. Intermediate passage causes line shifts and deformations<sup>6</sup> which could be prevented with the pulse technique.
- (2) The spectrum must have sufficient fine structure to give a high ratio of total sweep width to line width  $F/\Delta$  since this determines the achievable improvement [compare Eq. (3.12)].
- (3) The technical requirements are mainly concerned with the high field-frequency stability and with the availability of a suitable time averaging computer which must have a number of channels at least equal to  $2F/\Delta$  in order to give sufficient resolution and to cover the total frequency range of the spectrum.

These conditions are easily fulfilled for proton magnetic resonance in liquids. Here it is possible to gain up to a factor of 10 in sensitivity in a restricted time and up to a factor of 100 in time for a given sensitivity. There are some other systems where the same method could be used also, for example, boron resonance or deuterium resonance.

Fourier transform spectroscopy used in the described manner shows several side effects which have not been analyzed here in detail. The intensities of the resonance lines are often affected by Overhauser effects within the investigated spin system. Studies of these effects, both experimentally and theoretically, are in progress and will be published later. Using strong samples, maser effects due to radiation damping<sup>13</sup> can distort the spectrum. It should be emphasized that despite the presence of several transmitter frequencies no double or multiple resonance effects can occur. Furthermore, multiple quantum transitions do not occur either, irrespective of the rf field strength.<sup>2</sup>

<sup>13</sup> S. Bloom, *J. Appl. Phys.* **28**, 800 (1957); and A. Szöke and S. Meiboom, *Phys. Rev.* **113**, 585 (1959).